J Therm Anal Calorim (2016) 126:9–17
DOI 10.1007/s10973-016-5785-z

Thermal diffusivity characterization of bond-coat materials used for thermal barrier coatings

Grzegorz Moskal[1] · **Anna Jasik**[2]

Received: 14 November 2015 / Accepted: 17 August 2016 / Published online: 30 August 2016

Abstract Thermal barrier coatings (TBC) are the system build from ceramic insulation top-coat with internal bond-coat as an interlayer between ceramic and Ni-based superalloys substrate materials. The basic role of bond-coat is reduction of thermal strain between ceramic top-coat and metallic substrates. The second role is related to improving the oxidation resistance of metallic substrate. From thermal conductivity point of view, TBC's system is characterized by three different materials. Usually, bond-coats and Ni-based superalloys were treated as materials with similar thermal properties such as specific heat, thermal diffusivity and thermal conductivity. Actually those materials can exhibit much higher divergences than expected. The aim of this article was the characterization of thermal diffusivity of bond-coats material of NiCrAlY type in the form of powders, massive alloy (obtained during sintering in an actual pressure of 15 MPa, in vacuum of 3×10^{-6} MPa, and at temperature 1050 °C with 2 h of exposure in press), and coating after air plasma spraying. Those studies should get the answer on the question how different morphology and processes impact on thermal diffusivity level of the same material.

Keywords TBC · Bond-coats · NiCrAlY · Thermal diffusivity · Laser flasch analysis

✉ Grzegorz Moskal
grzegorz.moskal@polsl.pl

Anna Jasik
anna.jasik@polsl.pl

[1] Institute of Materials Science, Silesian University of Technology, ul. Krasińskiego 8, 40-019 Katowice, Poland

[2] Institute of Metals Technology, Silesian University of Technology, ul. Krasińskiego 8, 40-019 Katowice, Poland

Introduction

Thermal barrier coatings are the system of different type of layers where each of them has got other physical properties and role to play. The basic request of outer ceramic sub-layer is thermal insulation of substrate material (for example, made form Ni-based superalloys). The second important layer in TBC's system is bond-coat. Usually, this type of layer is formed by thermal spraying process of feedstock powder with precisely dedicated chemical composition on the substrate surface or by diffusional aluminization methods, where bond-coat is formed by diffusion and reaction between Ni and Al. The basic request of this layer is related to assurance of oxidation and corrosion resistance of substrate material and compensation of thermal expansion between ceramic outer layer and Ni-based substrate.

Additional structural element of TBC's system is thermally grown oxides (TGO) [1]. This zone is formed during high-temperature exposure of TBC's system and it is formed on the bond-coat surface. TGO zone is responsible for long-term durability (key factor is the thickness of this zone) of whole system, and its formation kinetic during oxidation is strongly dependent on temperature in area between ceramic insulation layer and bond-coat [2]. This temperature is dependent on the thickness and insulation properties of ceramic top layer, and it can be determined on the design stages of TBC's systems by numerical simulation [3–6]. But the accuracy of obtained simulation depends on the quality of the data used to simulation.

This article characterized the thermal diffusivity of bond-coat materials of NiCrAlY type usually used to bond-coat deposition by plasma spraying process. The influence of analysed materials' morphology on obtained, by laser-flash method, thermal diffusivity results is described.

Experimental

Ni–22Cr–10Al–Y (mass%) material in the three different morphological forms was the subject of the presented analysis. Spheroidal gas atomized Ni–22Cr–10Al–Y powder, in as-delivered condition, was an initial material used in the characterization of thermal diffusivity at temperature range from 25 to 1200 °C. Some details of microstructure of this powder were presented in position [7]. The second form of the same material was massive material (alloy) obtained by high-temperature sintering process of Ni–22Cr–10Al–Y powder in an actual pressure of 15 MPa, in vacuum of 3×10^{-6} MPa, and at temperature 1050 °C with 2 h of exposure in press. The last morphological form of Ni–22Cr–10Al–Y material used in this investigation is air plasma-sprayed coating described in as-sprayed condition and after oxidation test in earlier publications [8–10].

The range of investigation included short morphological characterization of materials such as their phase constituent descriptions by X-ray diffraction (XRD) method; characterization of microstructure by optical microscopy (OM); and scanning electron microscopy (SEM). Final analysis included characterization of thermal diffusivity by laser-flash analysis (LFA) at temperature range from 25 to 1200 °C. LFA 427 apparatus by Netzsch was used to characterize thermal diffusivity of analysed materials under an argon atmosphere on square or circular samples. In the case of powder, the pressed pastilles were used with the thickness ca. 2 mm and size of 10 × 10 mm. Similar thickness was the circular sintered specimen obtained in high-temperature press. The radius of this specimen was 10 mm. The last type of specimens was coated samples with size of 10 × 10 mm and thickness 1725 mm (1,50 mm with 0125 mm of NiCrAlY coating). The thickness of samples was measured by micrometre; additionally, SEM pictures with image analysis were used in the case of coating thickness measurement. Cowan's model was used for thermal diffusivity calculation in the case of single-layer analysis. This method gives the possibility to measure thermal diffusivity and heat capacity with high precision and is relatively simple in sample preparation and interpretation of results [11–14]. The analysed samples were placed in the sample carrier in such a way that their original surface (for example, rough top surface of NiCrAlY coating) was faced down. During the test, the laser flash illuminated this surface of specimen and the temperature distribution was measured on the opposite face.

XRD analysis of phase constituent in macroscale was made on X'Pert 3 Powder diffractometer (current 40 mA, voltage 40 kV) equipped with monochromator and strip detector. Microstructural characterization of powder and sinter was realized by SEM analysis (Hitachi S-4200 microscopy equipped with an EDS Thermo NORAN (System Six) and accelerating voltage of 25 kV) and optical microscopy of Nikon Eclipse E200 type.

Results

For better understanding of analysed problem, short information about morphology of used materials was firstly presented. The commercial powder of Ni–22Cr–10Al–Y type with spheroidal shape of granules as a result of gas atomization process was the first investigated materials. The morphological details of surfaces and internal structure of this powder are shown in Fig. 1. This shape is typical for atomization process of powder production. Internal structure revealed presence of dendritic form in granules' core, as an effect of rapid quenching during powder fabrication. Average chemical composition, obtained by EDS analysis from core area of presented granule, showed good accordance with supplier data. From homogeneity point of view, distribution of all elements was very regular without presence of participations or other microsegregation inside the granules. Phase constituent analysis by XRD method showed that main compounds detected in powder were as follows: Ni_3Al, Ni and probably NiAl (Fig. 2). There were no peaks assigned to phases including Y. From chemical point of view, detected compounds have statute of solid solutions of $(Ni,Cr)_3Al$ and Ni(Cr) type.

The second analysed material was obtained by the sintering method in high-temperature vacuum press. As a feedstock material, the same powder of Ni–22Cr–10Al–Y was used. In this case, the range of investigation included characterization of internal microstructure of sinter with chemical analysis in microareas and characterization of phase constituent as well.

Already, optical microscopy analysis revealed totally different types of obtained microstructure than in the case of powder's granules (Fig. 3a). Observed material has a multi-phase internal morphology with two-phase matrix and at least two different lighter and darker participations (Fig. 3b). Average chemical composition of sinter is very similar to that observed for feedstock powder.

Generally, matrix has been built from $(Ni,Cr)_3Al$, and Ni(Cr) phases with small amount of Al. In the case of participation, Ni(Cr)–Y with different levels of Y were detected. Phase analysis by XRD method revealed that detected diffraction peaks correspond to Ni_3Al and Ni phases. Additionally Ni–Y compounds of NiY and Ni_7Y type were confirmed as well. Probably, tertiary compounds from Ni–Y–Al system can exist as well (Fig. 4).

The last analysed morphological form of initial powder was plasma-sprayed coating deposited during standard process of this type of coating deposition. The thickness of

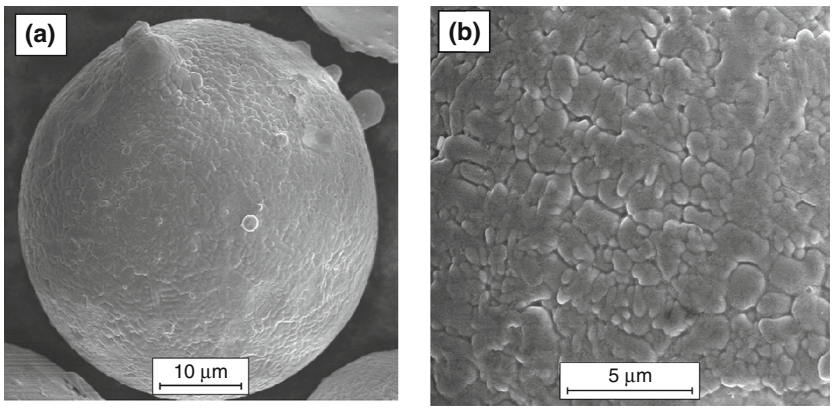

Fig. 1 Morphology of Ni–22Cr–10Al–Y powder: **a** top surface of granule, **b** internal structure in the core of granule

Mass%	Al	Cr	Ni	Y
av. comp.	10.37	21.90	66.73	1.00

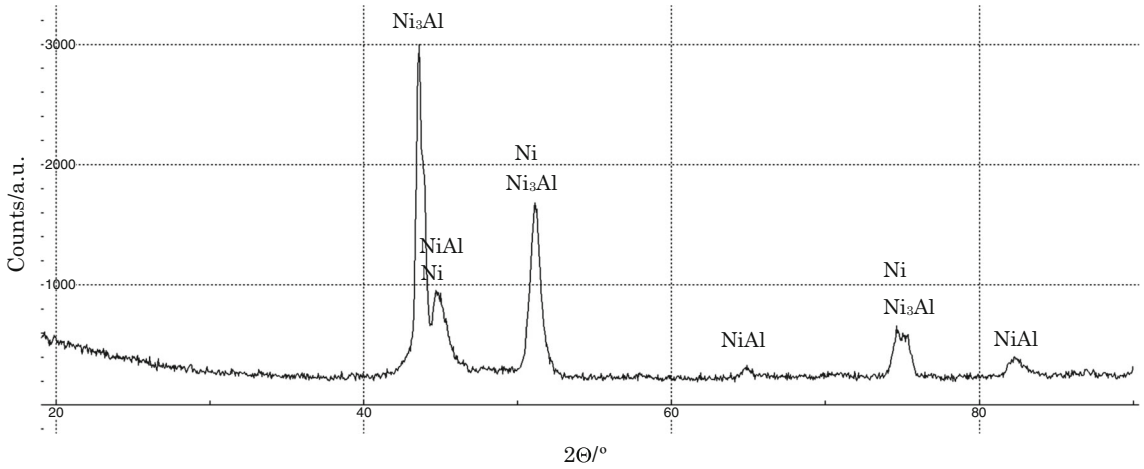

Fig. 2 XRD pattern of NiCrAlY powder

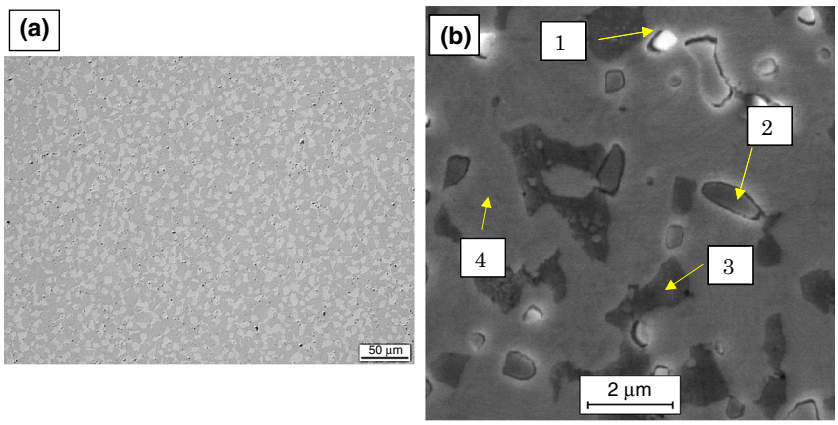

Fig. 3 Morphology of Ni–22Cr–10Al–Y powder: **a** OM picture, **b** SEM microstructure with places of EDS analysis

Mass%	Al	Cr	Ni	Y
Pt. 1	7.37	14.65	47.81	29.24
Pt. 2	4.83	8.14	45.26	41.15
Pt. 3	16.65	6.75	76.60	
Pt. 4	5.29	31.06	63.65	
av. comp.	8.63	22.61	67.58	1.17

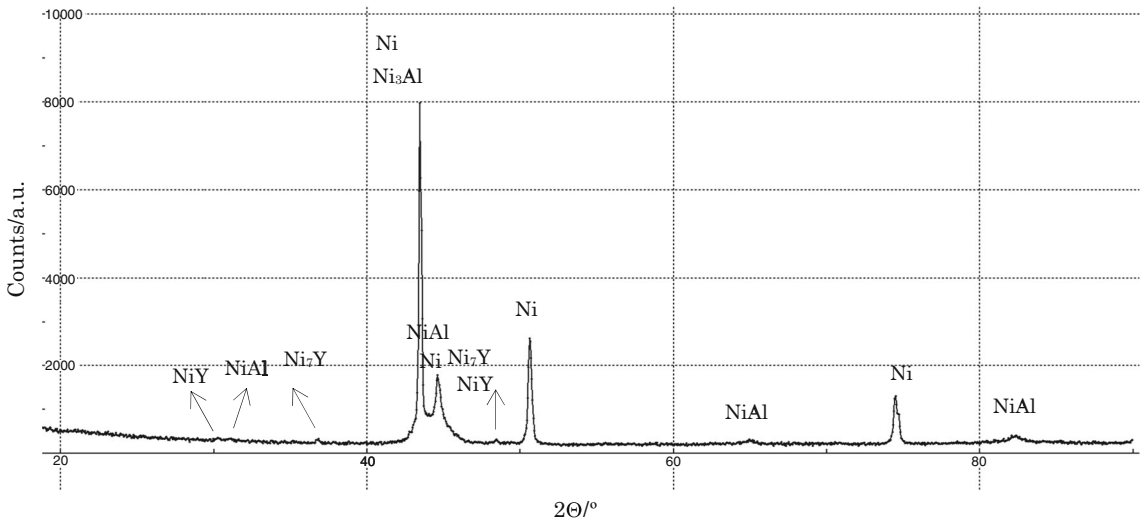

Fig. 4 XRD pattern of Ni–22Cr–10Al–Y sinter

coating was 125 μm. Its internal morphology is relatively most complicated in comparison with earlier investigated powder's granules and sinter. Observed differences are related with high temperature in plasma beam during the thermal spraying process.

OM picture of coating microstructure is shown in Fig. 5a, b. In this case, the brightness matrix consisted darker areas of other phases such as oxides (mainly Al_2O_3) or contaminations. Observed differences are related with high temperature in plasma beam during the thermal spraying process. Due to the characteristic of plasma spraying process, other structural elements such as non-melted spherical areas correspondent to feedstock granules can be observed as well. Though internal microstructure of coating was different, its phase constituent is very similar to this observed after sintering process (Fig. 6). Additionally, presence of oxides should be detected on diffraction pattern in this case.

The final goal of presented investigation was the characterization of thermal diffusivity of the same material in three different types of remanufacturing processes. Generally, during numerical simulations and characterization of temperature distribution as well as a stress development in TBC's system, the literature thermal data of bond-coats materials are usually used without considering its form (powder, massive alloy or real coating), as well as their porosity or other microstructural factors. The accuracy of data used to simulation has a strong influence on precision of obtained simulation, so the information about morphology and samples preparation is important from those points of view.

In next steps of investigation, data from laser-flash analysis were shown. First, information, presented in Fig. 7, concerns thermal diffusivity of substrate material In 625 Ni-based superalloy with and without plasma-sprayed bond-coats material of Ni–22Cr–10Al–Y type. Comparison data obtained for pressed Ni–22Cr–10Al–Y powder and sinter with the same chemical composition were shown.

These data showed that deposition of relatively thin bond-coat on the surface of In 625 substrate increase the value of thermal diffusivity in small range. The thickness of bond-coat was 125 μm and thickness of substrate was 1.5 mm, so the effect of thermal diffusivity enhancement was relatively strong. Thermal diffusivity of powders showed that high porosity of pressed pellet was the most important factor falsifying obtained results, but data obtained for NiCrAlY sinter are in accordance with obtained curve for In 625 alloy with NiCrAlY bond-coat. Only results for temperature higher than 900 °C showed decreasing tendency, which is the effect probably related to Ni–Y or Ni–Y–Al participation dissolution in solid solution of sinter.

The next analysis compared data of thermal diffusivity measurement of NiCrAlY-pressed powder and sinter (as earlier) and NiCrAlY coating obtained by grinding of substrate material In 625 to thickness ca. 125 μm which correspond to real thickness of bond-coat (Fig. 8). Data obtained for NiCrAlY coating after removing of substrate material are initially similar to that obtained for sinter, but at temperature higher than 200 °C, the difference is higher to the temperature 800 °C, when the level of thermal diffusivity rapidly increases to much higher value than for sintered material. This effect is related to very thin sample used for investigation and in consequence with time of measurement (so-called history of temperature). For thicker samples, this time was ca. 3000–5000 ms, when in this case it was ca. 30–50 ms. The minimal time of measurement suggested to obtain high accuracy results of

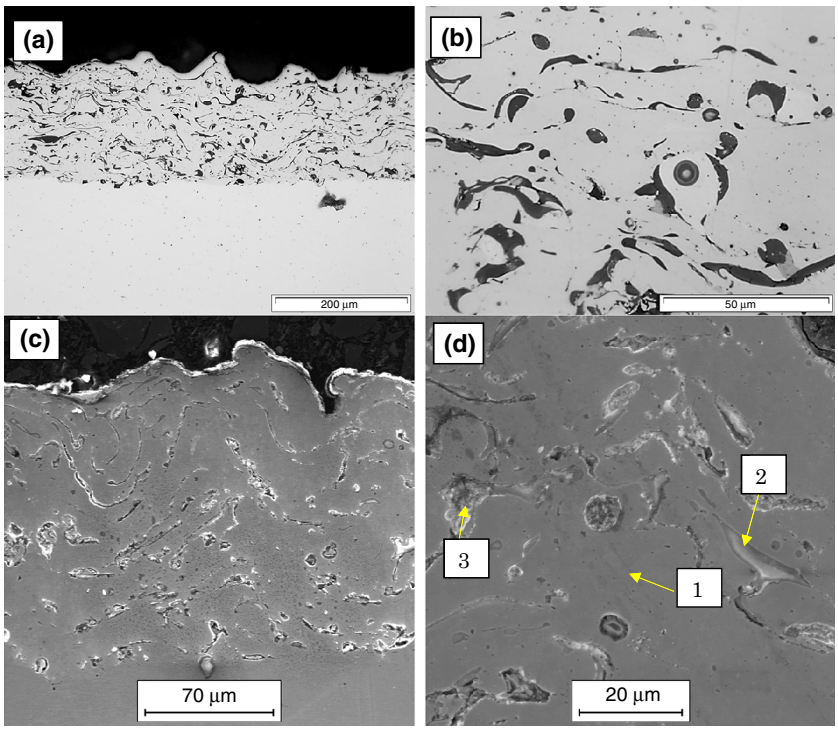

Fig. 5 Morphology of Ni–22Cr–10Al–Y coating: **a**, **c** main view of coatings, **b**, **d** internal structure of coatings with matrix and oxides as a result of plasma spraying process

Mass%	Al	Cr	Ni	Y
Pt. 1	8.2	22.3	69.2	0.3
Pt. 2	0.8	17.1	82.1	-
Pt. 3	40.1	31.7	25.1	3.1
av. comp.	5.00	22.55	71.54	0.91

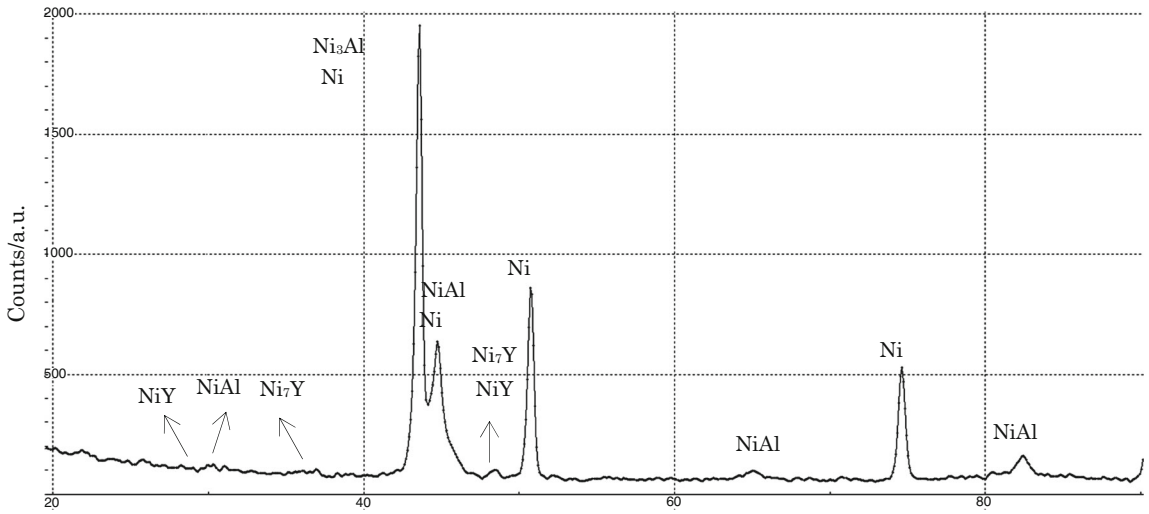

Fig. 6 XRD pattern of Ni-22Cr-10Al-Y plasma-sprayed coating

measurement should be no shorter than 50 ms. In consequence, those results are similar to those for sinter, but from methodical point of view, their accuracy is strongly discussed.

Another analysed factor was the characterization of thermal diffusivity results obtained by recalculation of data for In 625 with NiCrAlY bond-coat with application of models of Proteus software by Netzsch. The most problematic factor in this case is still relatively low thickness of bond-coat and small differences between thermal diffusivity of In 625 alloy and Ni–22Cr–10Al–Y alloys presented in Fig. 7. For this investigation, four available

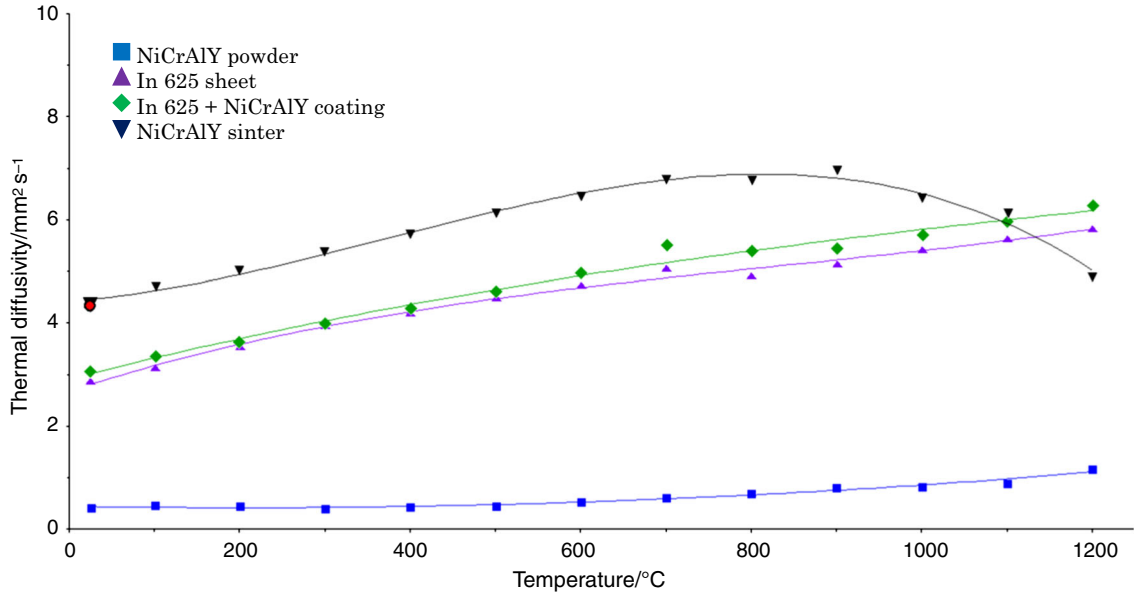

Fig. 7 Thermal diffusivity results for analysed materials

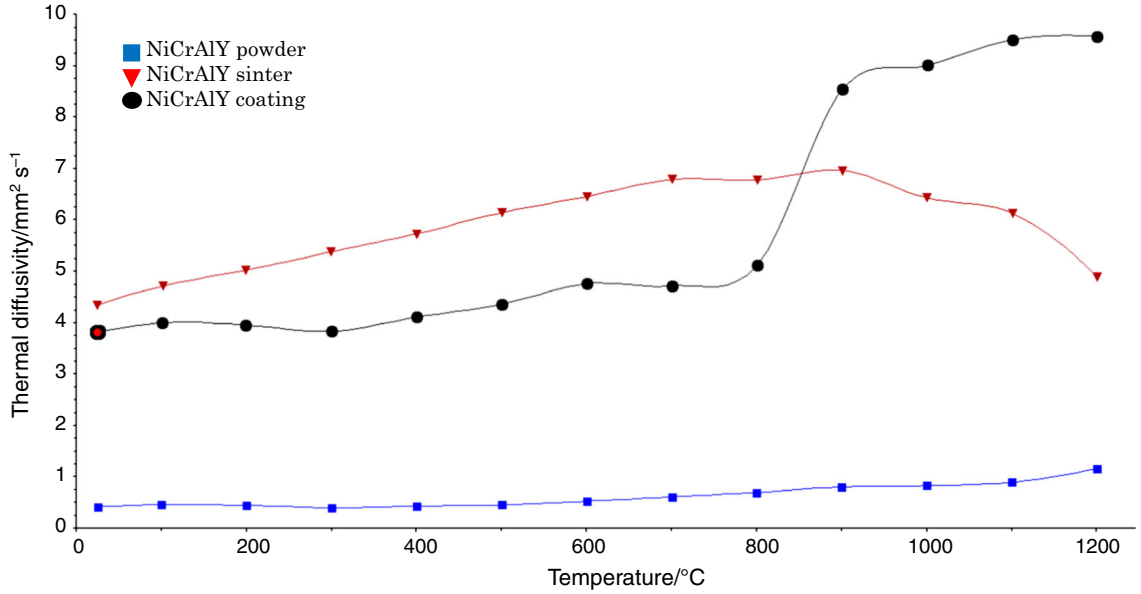

Fig. 8 Thermal diffusivity results for NiCrAlY-pressed powder, sinter and coating after removal of substrate material by grinding

models were used: 2L adiabatic with and without pulse correction and 2L heatloss with and without pulse correction.

Results for 2L adiabatic model with pulse correction are shown in Fig. 9 (data after recalculation for model without pulse correction were without any sense). In this case, good correlation is observed in temperature range 500–1000 °C with data for sintered NiCrAlY alloy. Good correlation was observed also for recalculated data obtained for 2L heatloss with and without pulse correction, but only to data for temperature range 25–500 °C. At higher temperature, this accordance does not exist. As explained earlier, those differences are related to low differences between thermal diffusion value of In 625 and NiCrAlY alloys and low thickness of bond-coat.

In Fig. 10, the samples of fitting process of real data from thermal diffusivity measurement to models available in Proteus software were shown. The quality of fit was very high, which suggests the high level of accuracy of obtained results.

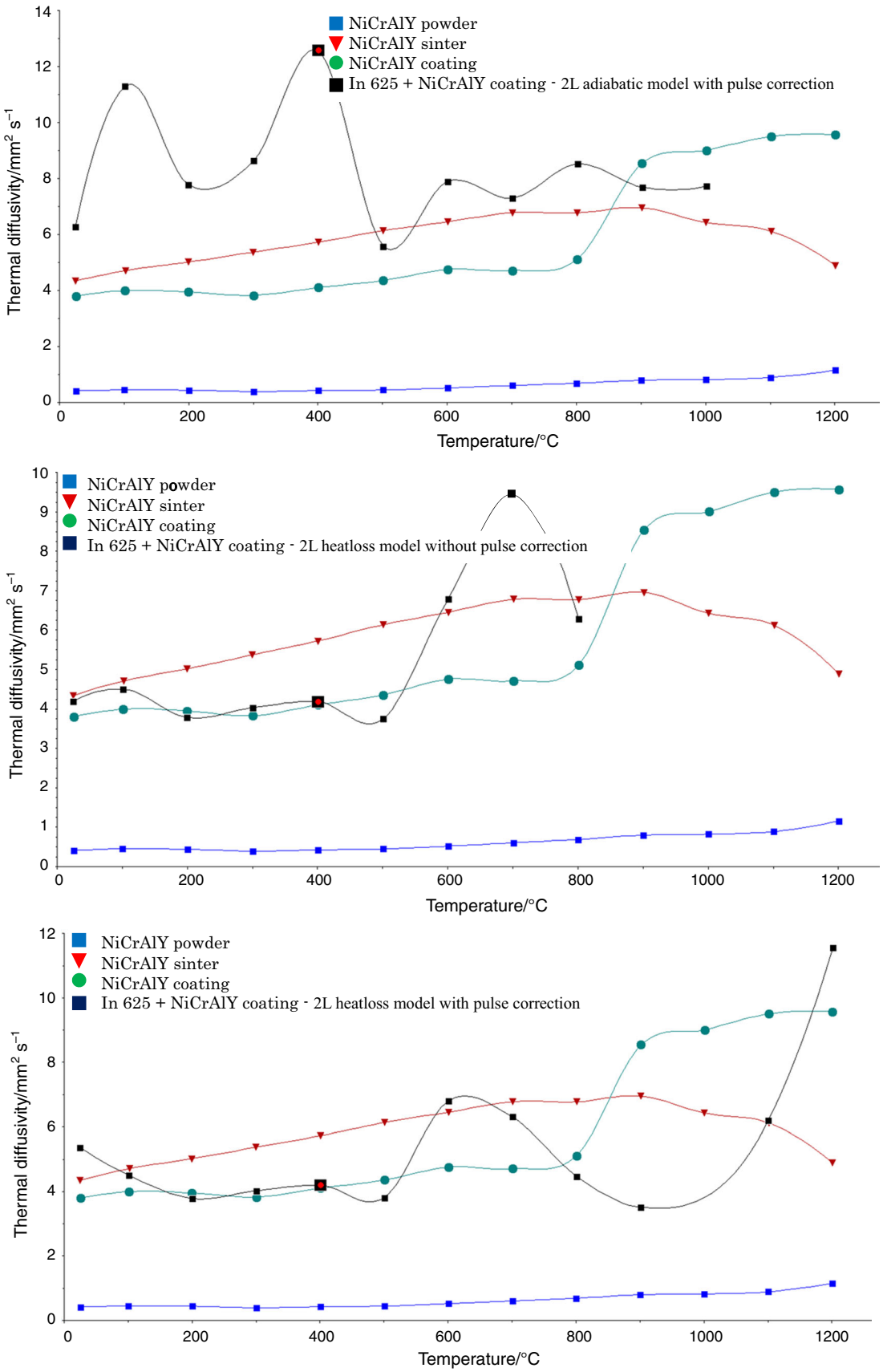

Fig. 9 Thermal diffusivity results for NiCrAlY after re-calculating with Proteus models

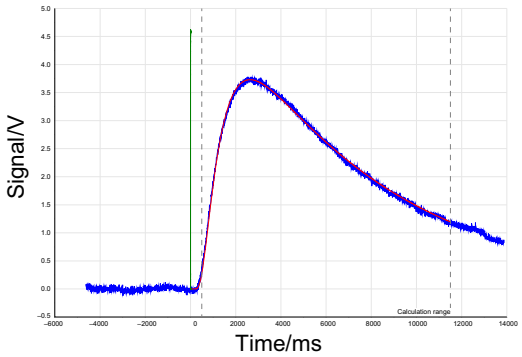

Fitting results for In 625 powder – Cape Lehman model – temperature 1200 ºC

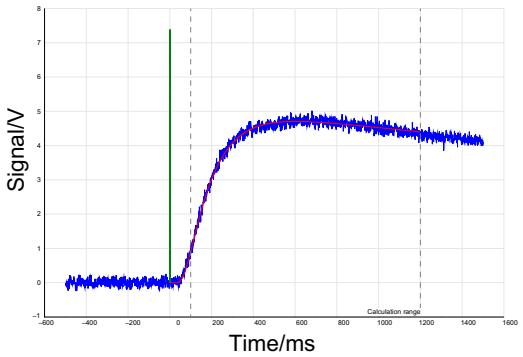

Fitting results for In 625 sinter – Cape Lehman model – temperature 1200 ºC

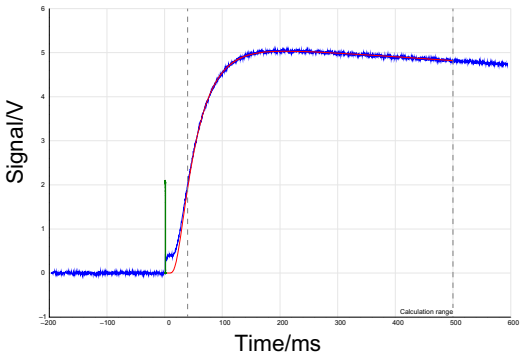

Fitting results for In 625 sheet without coating – Cape Lehman model – temperature 1200 ºC

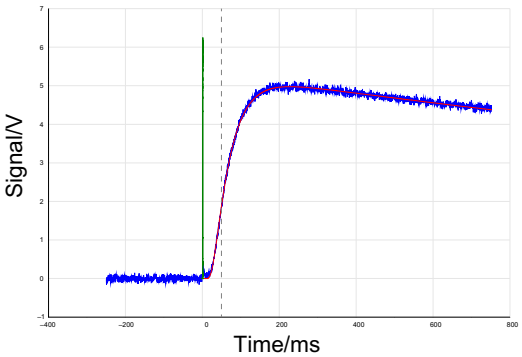

Fitting results for In 625 sheet with NiCrAlY coating – Cape Lehman model – temperature 1200 ºC

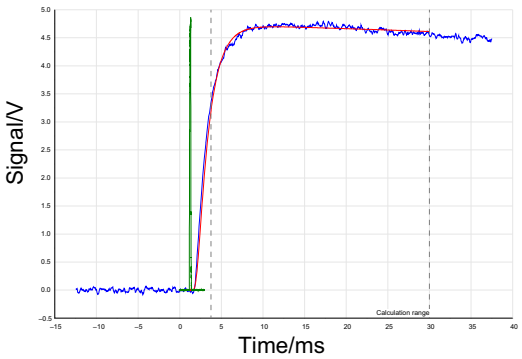

Fitting results for coating after substrate removing – Cape Lehman model – temperature 1200 ºC

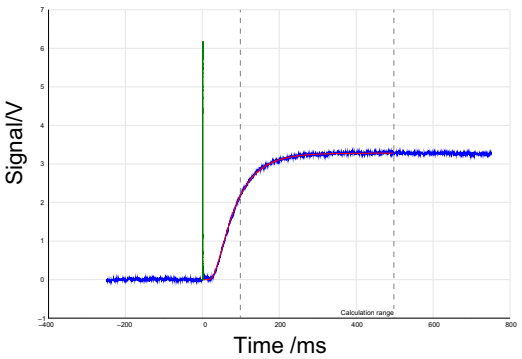

Fitting results for In 625 sheet with NiCrAlY coating – 2L adiabatic model – temperature 1000 ºC

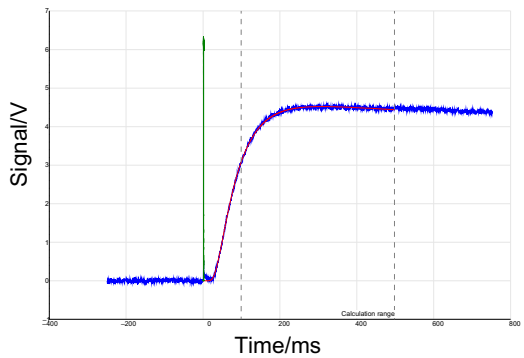

Fitting results for In 625 sheet with NiCrAlY coating – 2L heatloss without puls correction – temp.500 ºC

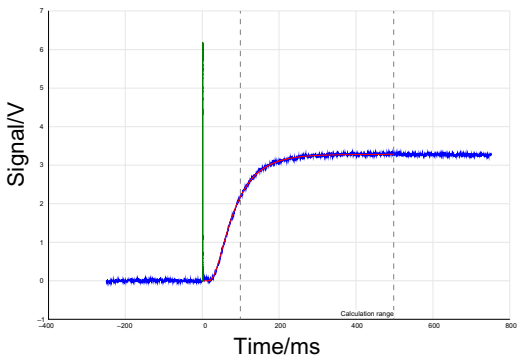

Fitting results for In 625 sheet with NiCrAlY coating – 2L heatloss with puls correction – temp.500 ºC

◀**Fig. 10** Samples of fitting process of real data from thermal diffusivity measurement to models available in Proteus software

Conclusions

Presented investigations showed that morphology of material NiCrAlY type used to analyse has a strong effect on thermal diffusivity values obtained during LFA test. It is an effect of differences in microstructure of materials in the form of powder, sinter (alloy) or coating, especially related to differences in phase constituent of those materials. In the case of NiCrAlY powder, only solid solution of Ni(Cr) and $(Ni,Cr)_3Al$ was detected (data obtained for pressed powder are incorrect mainly due to high level of porosity in pellets). After sintering process, additionally Ni–Y or/and Ni–Y–Al phases were detected, as well as for coating after plasma spraying. As a consequence, in those both cases, lower-level alloying elements in solid solution should be present, and the effect of thermal wave scattering should be lower as well. As a result, higher value of thermal diffusivity was observed for NiCrAlY sinter to 900 °C. At higher temperature, the effect of participation dissolution in matrix was observed and concentration of alloying elements in matrix was higher. This was reflected in higher value of thermal diffusivity at temperature higher than 900 °C. In the case of coating deposited by plasma spraying, additional microstructural element is the presence of oxides, as a result of metallic granules oxidation in plasma beam. This fact should decrease the value of thermal diffusivity of coating in comparison with sinter. Additional factor strengthening the problems with characterization of coating's thermal diffusivity is the very small thickness of this layer. The thickness of bond-coat layer is a also critical factor for application of different types of recalculating models used in this investigation, as well as the relative small differences between thermal diffusivity of In 625 substrate material and Ni–22Cr–10Al–Y powder. As a basic conclusion of presented investigations, it can be written as:

- The morphology of used materials has strong effect of accuracy of obtained data in laser-flash analysis;
- Observed differences in this value are related to differences in microstructure of material;
- The best thermal data with high accuracy can be obtained mainly by synthesis of specimens in the form of massive alloy (taking into considerations the microstructural differences related to other methods of final specimens preparations.

References

1. Swadźba L, Moskal G, Mendala B, Hetmańczyk M. Characterization of microstructure and properties of TBC systems with gradient of chemical composition and porosity. Arch Metall Mater. 2008;53:945–9.
2. Moskal G, Swadźba L, Mendala B, Góral M, Hetmańczyk M. Degradation of the TBC system during the static oxidation test. J Microsc Oxford. 2010;237:450–5.
3. Antou G, Montavon G, Hlawka F, et al. Modification of thermal barrier coating architecture by in situ laser remelting. J Eur Ceram Soc. 2006;26:3583–97.
4. Petorak C, Ilavsky J, Wang H, et al. Microstructural evolution of 7 wt% Y_2O_3–ZrO_2 thermal barrier coatings due to stress relaxation at elevated temperatures and the concomitant changes in thermal conductivity. Surf Coat Technol. 2010;205:57–8.
5. Renteria AF, Saruhan B, Schulz U, et al. Effect of morphology on thermal conductivity of EB-PVD PYSZ TBC's. Surf Coat Technol. 2006;201:2611–9.
6. Ratzer-Scheibe HJ, Schulz U, Krell T. The effect of coating thickness on the thermal conductivity of EB-PVD PYSZ thermal barrier coatings. Surf Coat Technol. 2006;200:5636–8.
7. Moskal G. Microstructural characterization of Ni(Co)CrAlY powders designed for thermal spraying of bondcoat for TBC systems. Solid State Phenom. 2013;203–204:435–8.
8. Moskal G. Thermal barrier coatings: characteristics of microstructure and properties, generation and directions of development of bond. J Achiev Mater Manuf Eng. 2009;37:323–8.
9. Moskal G, Niemiec D. Influence of surface condition on oxides layer morphology on NiCrAlY coating during oxidation at temperature 1000°C and 1100°C. Solid State Phenom. 2015;227:385–8.
10. Niemiec D, Moskal G, Mikuśkiewicz M, Mościcki A, Kałamarz P, Carski Ł. Influence of top-surface condition on oxidation resistance of NiCrAlY coating on Inconel 625 alloy. Ochr Przed Kor. 2014;7:255–6.
11. Rutkowski P, Klimczyk P, Jaworska L, Stobierski L, Dubiel A. Thermal properties of pressure sintered alumina–graphene composites. J Therm Anal Calorim. 2015;122:105–9. doi:10.1007/s10973-015-4694-x.
12. Kövér M, Behúlová M, Drienovský M, Motyčka P. Determination of the specific heat using laser flash apparatus. J Therm Anal Calorim. 2015;122:151–5.
13. Rutkowski P, Stobierski L, Górny G. Thermal stability and conductivity of hot-pressed Si_3N_4–graphene composites. J Therm Anal Calorim. 2014;116:321–8.
14. Parker WJ, Jenkins RJ, Butler CP, Abbott GL. Flash method of determining thermal diffusivity, heat capacity and thermal conductivity. J Appl Phys. 1961;32:1679.